Carbon Nanotube-enhanced Thermal Destruction of Cancer Cells in a Noninvasive Radiofrequency Field

Christopher J. Gannon, MD[1]
Paul Cherukuri, PhD[1,2]
Boris I. Yakobson, PhD[3,4]
Laurent Cognet, PhD[5,6]
John S. Kanzius[7]
Carter Kittrell, PhD[3,8]
R. Bruce Weisman, PhD[3,5]
Matteo Pasquali, PhD[3,5,8,9]
Howard K. Schmidt, PhD[5,8]
Richard E. Smalley, PhD[3,5,8†]
Steven A. Curley, MD[1,4]

[1] Department of Surgical Oncology, The University of Texas M. D. Anderson Cancer Center, Houston, Texas.

[2] Department of Experimental Therapeutics, The University of Texas M. D. Anderson Cancer Center, Houston, Texas.

[3] Department of Chemistry, Rice University, Houston, Texas.

[4] Mechanical Engineering and Materials Science, Rice University, Houston, Texas.

[5] Center for Biological and Environmental Nanotechnology, Rice University, Houston, Texas.

[6] Center of Optical and Hertzian Molecular Physics, National Center for Scientific Research, Bordeaux University, Bordeaux, France.

[7] ThermMed LLC, Erie, Pennsylvania.

[8] Carbon Nanotechnology Laboratory, Rice University, Houston, Texas.

[9] Department of Chemical and Biomolecular Engineering, Rice University, Houston, Texas.

Supported by American Association of Cancer Research Littlefield Grant (to C.J.G. and S.A.C.), by the National Aeronautics and Space Administration and the Alliance for NanoHealth (to P.C., R.E.S., and H.K.S.), by the National Science Foundation and the Center for Biological and Environmental Nanotechnology (to B.I.Y., L.C., M.P., R.B.W., and H.K.S.), and by the Fulbright Foundation (L.C.).

J.S.K. is the inventor of the radiofrequency field using nanoparticles.

BACKGROUND. Single-walled carbon nanotubes (SWNTs) have remarkable physicochemical properties that may have several medical applications. The authors have discovered a novel property of SWNTs—heat release in a radiofrequency (RF) field—that they hypothesized may be used to produce thermal cytotoxicity in malignant cells.

METHODS. Functionalized, water-soluble SWNTs were exposed to a noninvasive, 13.56-megahertz RF field, and heating characteristics were measured with infrared thermography. Three human cancer cell lines were incubated with various concentrations of SWNTs and then treated in the RF field. Cytotoxicity was measured by fluorescence-activated cell sorting. Hepatic VX2 tumors in rabbits were injected with SWNTs or with control solutions and were treated in the RF field. Tumors were harvested 48 hours later to assess viability.

RESULTS. The RF field induced efficient heating of aqueous suspensions of SWNTs. This phenomenon was used to produce a noninvasive, selective, and SWNT concentration-dependent thermal destruction in vitro of human cancer cells that contained internalized SWNTs. Direct intratumoral injection of SWNTs in vivo followed by immediate RF field treatment was tolerated well by rabbits bearing hepatic VX2 tumors. At 48 hours, all SWNT-treated tumors demonstrated complete necrosis, whereas control tumors that were treated with RF without SWNTs remained completely viable. Tumors that were injected with SWNTs but were not treated with RF also were viable.

CONCLUSIONS. The current results suggested that SWNTs targeted to cancer cells may allow noninvasive RF field treatments to produce lethal thermal injury to the malignant cells. Now, the authors are developing SWNTs coupled with cancer cell-targeting agents to enhance SWNT uptake by cancer cells while limiting uptake by normal cells. ***Cancer*** **2007;110:2654–65.** © *2007 American Cancer Society.*

KEYWORDS: carbon nanotubes, radiofrequency, thermal cytotoxicity, cancer cells.

A noninvasive approach with the potential to treat many types of cancers effectively with minimal or no toxic effects to normal cells would be highly beneficial. Toward this objective, we combined a radiofrequency (RF) field-generating system with single-walled carbon nanotubes (SWNTs), which act efficiently to convert RF irra-

The first two authors contributed equally to this article.

†Deceased.

We thank K. Ash for assistance in preparing the article.

Address for reprints: Steven A. Curley, MD, Department of Surgical Oncology, Unit 444, The University of Texas M. D. Anderson Cancer Center, 1400 Holcombe Boulevard, Houston, TX 77030; Fax: (713) 745-5235; E-mail: scurley@mdanderson.org

Received August 20, 2007; accepted September 19, 2007.

DOI 10.1002/cncr.23155
Published online 24 October 2007 in Wiley InterScience (www.interscience.wiley.com).

diation into heat. Although, today, RF ablation (RFA) is used in clinical practice to treat some malignant tumors, it suffers from serious drawbacks.[1] RFA currently is an invasive treatment that requires the insertion of needle electrodes directly into the tumor(s) to be treated; incomplete tumor destruction occurs in from 5% to 40% of the treated lesions; the treatment is nonspecific and induces thermal necrosis in both malignant and normal tissues surrounding the needle electrode; complications arise in up to 10% of patients related to thermal injury to normal tissues; and invasive RFA is limited to the treatment of tumors in only a few organ sites (liver, kidney, breast, lung, bone). Conversely, it is known that the tissue penetration by RF energy fields is excellent.[2] Thus, noninvasive RF treatment of malignant tumors at any site in the body should be possible if agents that convert RF energy into heat can be delivered to the malignant cells.

Biomedical applications for SWNTs are being investigated actively because of their useful combination of size and physicochemical properties.[3–8] In cancer patients, SWNTs have potential roles in delivering pharmacologic agents, diagnostic imaging agents, DNA, silent interfering RNA, oligonucleotides, and proteins to detect or treat cancer cells.[9–11] Roughly 66% of SWNTs are high-mobility, direct band-gap seimiconductors[7] that fluoresce in the near infrared (NIR);[8] the rest are metallic conductors capable of carrying exceptional current densities.[5] Given the unique electrical and chemical properties of SWNTs, we hypothesized that exposure to a focused external RF field would lead to significant heat release by the SWNTs, allowing them to serve directly as an anticancer therapeutic agent. We report herein that exposure of intracellular SWNTs in vitro and intratumoral SWNTs in vivo to a noninvasive, focused RF field produces lethal heating of malignant cells.

MATERIALS AND METHODS

Functionalized SWNTs

Sterile CoMoCAT SWNTs functionalized with Kentera (Zyvex Corp, Richardson, Tex) were obtained at a standard concentration of 500 mg/L. Kentera is a polymer based on polyphenylene ethynylene (PPE). The phenyl groups of the PPE are linked to form a rigid, conjugated polymer that functionalizes SWNTs through π–π stacking (noncovalent interaction). Sterility of the SWNT solutions was assured by a 20-minute exposure to ultraviolet irradiation. Characterization of the Kentera SWNT solution to assess for individual versus clusters of SWNTs was performed by atomic force microscopy (AFM) at 633 nm. A 20-μL aliquot of Kentera SWNTs was spun cast onto mica for AFM. Purity of the SWNT solutions and analysis of metal content was performed by inductively coupled plasma-mass spectroscopy. The mass spectroscopy analysis of the Kentera SWNTs used for all of our studies shows Mo, 58 parts per million (ppm) (0.0058%); Co, 3ppm; Fe, 0.2 ppm; and Ti, 0.1 ppm. Raman spectroscopy was performed and confirmed the presence of the signal intensity peaks that were observed with individual SWNTs (data not shown). In all suspensions, the mass ratio of SWNTs to Kentera was 1:1.

External RF Generator/Coupling System

A variable power 0- to 2-kilowatt, 13.56-megahertz (MHz) RF signal generator (Therm Med LLC, Erie, Pa) was built to specifications for use in these experiments. The RF generator is connected to a high Q coupling system (Therm Med LLC) that has a transmitting (Tx) head, a receiving (Rx) head, and coupling circuitry. The Tx and Rx heads and the contained coupling circuitry are mounted on a swivel bracket, allowing the RF field to be oriented in either a horizontal or vertical direction. The distance between the heads is adjustable, and the RF field is generated between the Tx and Rx heads. The coaxial coupling circuitry in the Tx and Rx heads produces a focused electromagnetic field with a useful diameter of 30 cm and with a peak intensity of 7 cm from the central axis of the Tx and Rx heads. Each time the RF field is activated, the heads are checked, and the coupling circuit is fine-tuned to assure that there is no power reflected back through the coupling circuit.

The electromagnetic field strength between the Tx head and Rx head was established in a Farraday-shielded room to exclude any interference from external RF sources. The field strength was measured at low power using an isotropic field monitor and probe (models FM2004 and FP2000, respectively; Amplifier Research Inc., Souderton, Pa); a Hewlett-Packard Spectrum Analyzer (model 8566B; Agilent, Santa Clara, Calif) was connected concomitantly to the system through a directional coupler to measure transmitted power accurately. The field strengths measured at low generator output powers were then used to estimate field strengths at the various RF generator output powers that were used in our experimental studies.

Thermal Effect of RF Field on Functionalized SWNTs

Serial dilutions of Kentera SWNTs were used to assess concentration dependency to heat-deionized water. Several concentrations of functionalized SWNTs were diluted serially in deionized water and placed in a 1.5-mL, circular quartz cuvette (height,

15 mm; diameter, 10 mm) located between the Tx and Rx heads of the RF generator using a nonmetallic, nonconductive Teflon holder. The samples were located at the mid plane of the working volume and were positioned radially to capture the maximum electric field potential. The Tx and Rx heads were spaced with a 7.5-cm air gap for these experiments. Temperature in the Kentera SWNT solutions, in solutions of Kentera without SWNTs, and in water alone were measured continuously before activating the RF field, during the entire period of RF field activation, and for 2 minutes after RF field shutdown by using a thermoelectrically cooled, Indium antimonide, focal plane array IR camera (Amber Engineering, Goleta, Calif). IR video was captured at 30 frames per second by using iMovie software (Apple, Cupertino, Calif), and all temperature measurements were performed in triplicate.

Human Cancer Cell Lines

HepG2 and Hep3B hepatocellular cancer cells and Panc-1 pancreatic adenocarcinoma cells (American TypeCulture Collection, Bethesda, Md) were cultured in Dulbecco modified Eagle medium (DMEM) with 10% fetal calf serum (FCS) plus penicillin/streptomycin at 37°C under standard atmospheric conditions. For experiments, each cell line was used only from passages 2 through 9. For cell proliferation assays, cells were grown to confluence in 96-well culture plates. For cytotoxicity studies with or without RF field treatment, cells were grown to near confluence in 60-mm glass culture dishes.

Cell Proliferation Assay

The 3 human cancer cell lines were grown to near confluence in 96-well plates. Media was aspirated from the cells, and media containing various concentrations of functionalized SWNTs or control media was added to the cell lines. Cell culture plates were returned to the incubator for 24 hours at 37°C. Fifty microliters of 3-(4,5-dimethylthiazol-2-yl)-2, 5-diphenyltetrazolium bromide (MTT) (Sigma-Aldrich Corp., St. Louis, Mo) were added to each of the 96 wells, and the plates were incubated for an additional 4 hours at 37°C. The cell culture plates were then centrifuged at 1500 revolutions per minute (rpm) for 5 minutes, the supernatant fluids were aspirated, and the cells were then solubilized by adding 100 μL of dimethyl sulfoxide to each well. Absorbance was read on an automated, multiwell, plate-scanning spectrophotometer at 570 nm and recorded. Each concentration was repeated in triplicate with 5 wells in each group.

Brightfield and NIR Microscopy

Cells were grown on glass coverslips in 60-mm glass dishes for NIR microscopy. Twenty-four hours after addition of SWNTs to the human cancer cell cultures, the media was aspirated from the cultures, and the cells were washed with phosphate-buffered saline (PBS) and resuspended in fresh media without SWNTs. To confirm intracellular localization of SWNTs, acid washing (pH 2.0) was performed on cell cultures to quench external SWNT emission and to remove any SWNTs adsorbed on the cell surfaces. Acidic media was aspirated and discarded, and fresh media was added for fluorescence imaging. Coverslips were mounted in thermoregulated slide holders to maintain a temperature of 37°C during fluorescence imaging. The cellular location of SWNTs was measured by both brightfield and NIR microscopy. NIR images of SWNTs from within cancer cells were measured by using a cryogenically cooled 320 × 256 pixel image Indium gallium arsenide detector array (model OMA-V 2D; Roper Scientific, Trenton, NJ). A ×60 oil-immersion objective was used for obtaining images, and the laser spot size was focused from 50 to 100 μm in greatest dimension (100–200 pixels under ×60 magnification). An excitation laser at 658 nm was used with a 946-nm long pass-blocking filter in the detection path.

Assessment of Cytotoxicity

The 3 human cancer cell lines were grown to near confluence in 60-mm culture dishes. Media was aspirated; fresh media containing various concentrations of Kentera SWNTs, Kentera alone, or media alone was added to the cells, and they were incubated for an additional 24 hours at 37°C. After 24 hours, the media was aspirated, and the cells were washed 3 times with PBS to remove any Kentera SWNTs or Kentera that was not taken up by the cells. Three milliliters of fresh media without SWNTs were added to each culture plate, and then the culture dishes were placed individually on a nonconductive Teflon holder between the Tx and Rx heads of the RF generator. The heads were oriented in a vertical direction with a 7.5-cm space between the heads. Then, the cells were exposed to a 13.56-MHz external RF field at 800 W for 1 or 2 minutes. After the prescribed period of RF field exposure, the culture dishes were returned to the incubator for an additional 18 hours at 37°C. Cells were harvested from the culture dishes by trypsinization, washed with PBS, and centrifuged at 1500 rpm for 5 minutes. The cell pellet was resuspended during gentle vortexing and while adding 5 mL of 95% ethanol. Cells were fixed overnight at room temperature and then stored at 4° until they

were ready for staining. For staining with propidium iodide (PI) (Sigma-Aldrich Corp.), cells were centrifuged in the fixative at 1500 rpm for 5 minutes and then resuspended in a Tris buffer solution (stock solution: 24 g Tris, 12 g NaCl, 168 mL 1N HCl in a total volume of 2 L [pH 7.4]). The cell pellets were resuspended in 500 μL of Tris buffer and 1 mL of PI (500 μg/mL in water were added). Thirty minutes before flow cytometric analysis, 100 μL of RNase (1 mg/mL and DNase-free; Sigma-Aldrich Corp.) were added, and the fixed cells were incubated at 37°C. Cell viability was assessed by adding the PI-stained cells to a fluorescence-activated cell sorter (FACS) Calibur unit (BD Biosciences, San Jose, Calif), and cell cycle proportions and cell viability were assessed with Cell Quest Pro software (BD Biosciences). All experiments were performed in quadruplicate.

Tumor-bearing Animal Model

All animal experiments were performed under a protocol that was reviewed and approved by the Institutional Animal Care and Utilization Committee at the University of Texas M. D. Anderson Cancer Center. VX2 tumor cells were grown in DMEM plus 10% FCS to confluence. The cells were harvested, washed, and resuspended in sterile PBS. One milliliter of the VX2 tumor solution was injected into each flank of 2 adult New Zealand white rabbits (3.0–3.5 kg). When tumors in the flanks of the donor rabbits reached a greatest dimension of 2.5 to 3.0 cm, the tumors were harvested under sterile condition and cut into 1-mm cubes. Under general endotracheal anesthesia, a 2-cm upper midline laparotomy incision was made in adult New Zealand white rabbits. An incision 1 mm long was made in the capsule of a right liver segment with a No. 11 scalpel blade, and a single cube of VX2 tumor was inserted into the liver parenchyma. The abdominal wall incisions were then closed under sterile conditions, and the animals were recovered from anesthesia. Two weeks later, under general endotracheal anesthesia, a repeat midline laparotomy procedure was performed, and the resulting intrahepatic VX2 tumor (greatest dimension, 1.0–1.3 cm) was injected directly with either a 1.0-mL solution of Kentera SWNTs (500 mg/L) with 100 μg of epinephrine in 4 animals or with 1.0 mL of control solution consisting of Kentera polymer (500 mg/L) and 100 μg of epinephrine (no SWNTs) in 4 animals. An additional 4 animals underwent intratumoral injection of Kentera SWNTs (500 mg/L) with epinephrine and served as a control group that was not treated with RF. Epinephrine was added to the SWNT and control solutions to produce transient intratumoral vasoconstriction to reduce diffusion of SWNTs or control solution out of the tumor. A final control group of 4 animals underwent RF field treatment of the liver tumors without injection of SWNTs or control solution into the tumors. The 12 animals that were to receive RF treatment were placed individually on a nonmetallic, nonconductive Teflon platform between the Tx and Rx heads of the RF generator with 10 cm of spacing between the heads. The Tx and Rx heads were oriented in a vertical configuration. Each animal was positioned so the hepatic tumor was located at the mid plane of the working volume to capture the maximum electric field potential. The RF field was activated and tuned, and each animal was treated for 2 minutes with RF at 600 W; then, the laparotomy incision was closed by using sterile technique, and the animals were allowed to recover from the treatment. Forty-eight hours later, the animals were euthanized, and the liver and other tissues were harvested and evaluated to assess for any evidence of thermal injury. The liver and VX2 tumor were fixed in 10% formalin. Tissue samples were cut, embedded in paraffin, then prepared for histologic assessment with hematoxylin and eosin staining and with terminal deoxynucleotidyl transferase biotin-deoxyuridine triphosphate nick-end labeling for apoptosis and viability according to the standard protocol provided by Promega (Promega Corp., Madison, Wis).

Statistical Analysis

Differences between experimental groups (with experiments performed in triplicate) were determined by using an analysis of variance with Statistica software (StatSoft Inc, Tulsa, Okla). A significant difference between groups was defined as $P < .05$.

RESULTS

RF-induced Heating of SWNT Suspensions

We used SWNTs functionalized noncovalently with Kentera (Zyvex; Richardson, Tex), which is a nonionic, biocompatible polymer that does not substantially alter the electronic properties of the nanotube.[12] We first characterized the heating rates and field dependence of the SWNTs, and we tested 5 different concentrations of aqueous SWNT suspensions (5 mg/L, 50 mg/L, 125 mg/L, 250 mg/L, and 500 mg/L) in a 1.5-mL quartz cuvette. Each suspension was placed in an experimental, focused, 13.56-MHz RF signal generator (ThermMed LLC, Erie, Pa; US Patent nos. US2006/0190063 A1, US2005/02511233 A1, and US2005/0251234 A1 and World Intellectual Property Organization WO 2007/027614) that included coupling circuitry housed in transmission (Tx) and

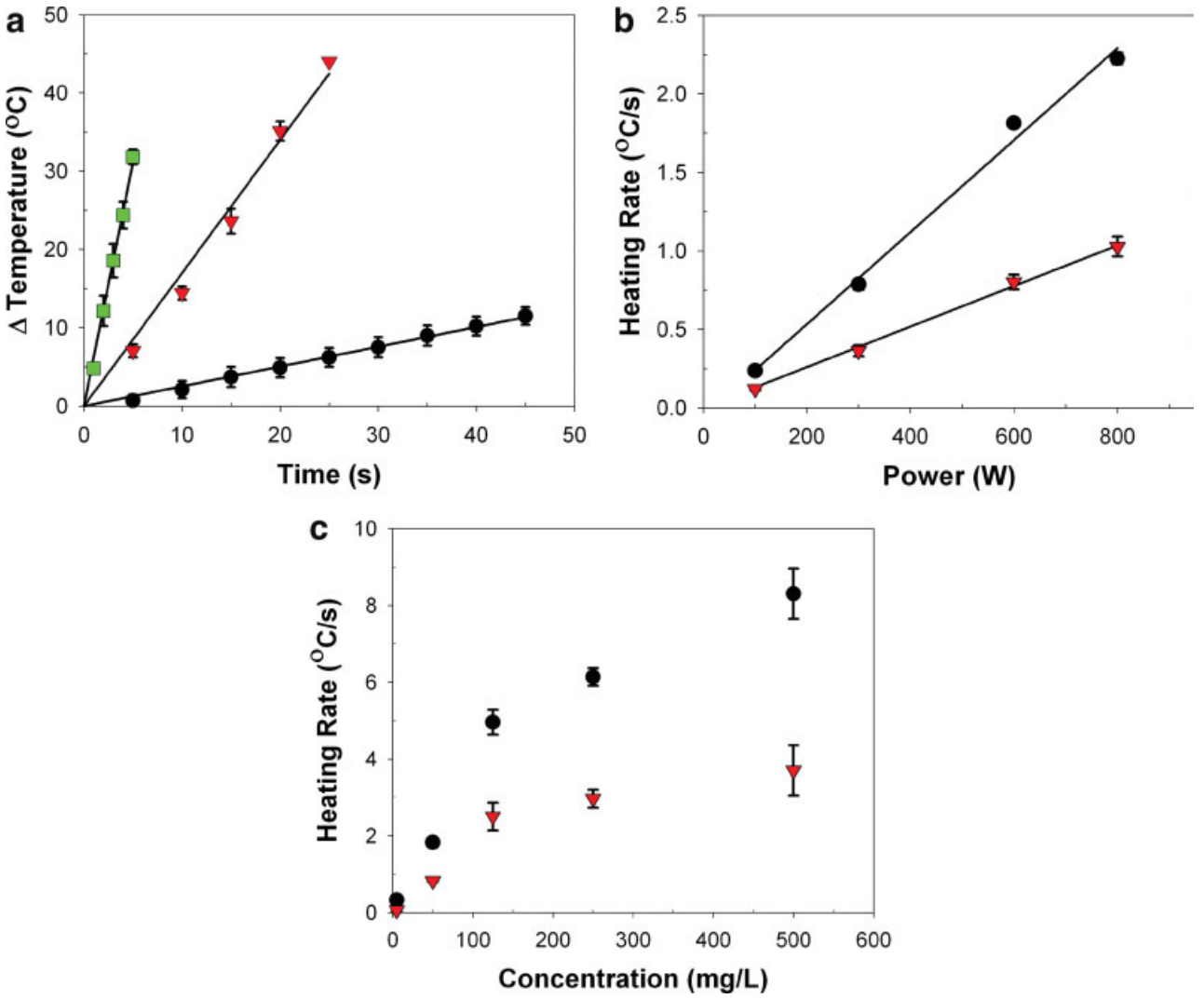

FIGURE 1. (a) Aqueous single-walled carbon nanotube (SWNT) suspensions under 600 watts (W) of radiofrequency (RF) generator output power exhibit a linear increase in temperature over time in seconds (s) (initial temperature, ≈25°C). Shown are the average suspension temperatures for 5 mg/L Kentera control samples (no SWNTs; dots) and Kentera SWNT suspensions for 50 mg/L (triangles) and for 250 mg/L (squares). (b) Heating rate of 50 mg/L of Kentera SWNT suspensions (dots) under RF generator output powers of 100 W, 300 W, 600 W, and 800 W. Suspensions exhibited linear heating with increasing RF power. Also shown is the SWNT heating rate (triangles), which was calculated by subtracting the background heating caused by the Kentera control suspensions. (c) Heating rate of Kentera SWNT suspensions under 600 W of RF generator output power with concentrations of 5 mg/L, 50 mg/L, 125 mg/L, 250 mg/L, and 500 mg/L. Suspensions exhibited nonlinear heating rates with increasing SWNT concentration. Shown are the averages of the heating rates for Kentera SWNTs (dots) and the calculated SWNT heating contribution (triangles). Note: In panel c, errors bars may be smaller than the symbols.

receiving (Rx) heads. This RF system produces a concentrated electromagnetic field between the Tx head and the Rx head. A 13.56-MHz signal generator was used because it is an industrial, scientific, and medical working frequency allocated by the Federal Communications Commission; furthermore, it was demonstrated previously that this frequency produces minimal tissue heating related to the specific absorption rate of electromagnetic radiation in mammalian testing.[13]

We observed that these noncovalently suspended SWNTs were very effective at converting RF energy into heat. With our instrument, output powers of 400 W, 600 W, 800 W, and 1000 W were used, yielding a maximum estimated electric field strength 2.5 cm from the Tx head of 10.1 kilovolts (kV)/m, 12.4 kV/m, 14.3 kV/m, and 16.0 kV/m, respectively. We determined that the lowest SWNT concentration that produced enhanced bulk heating, compared with a reference sample of deionized water alone, was

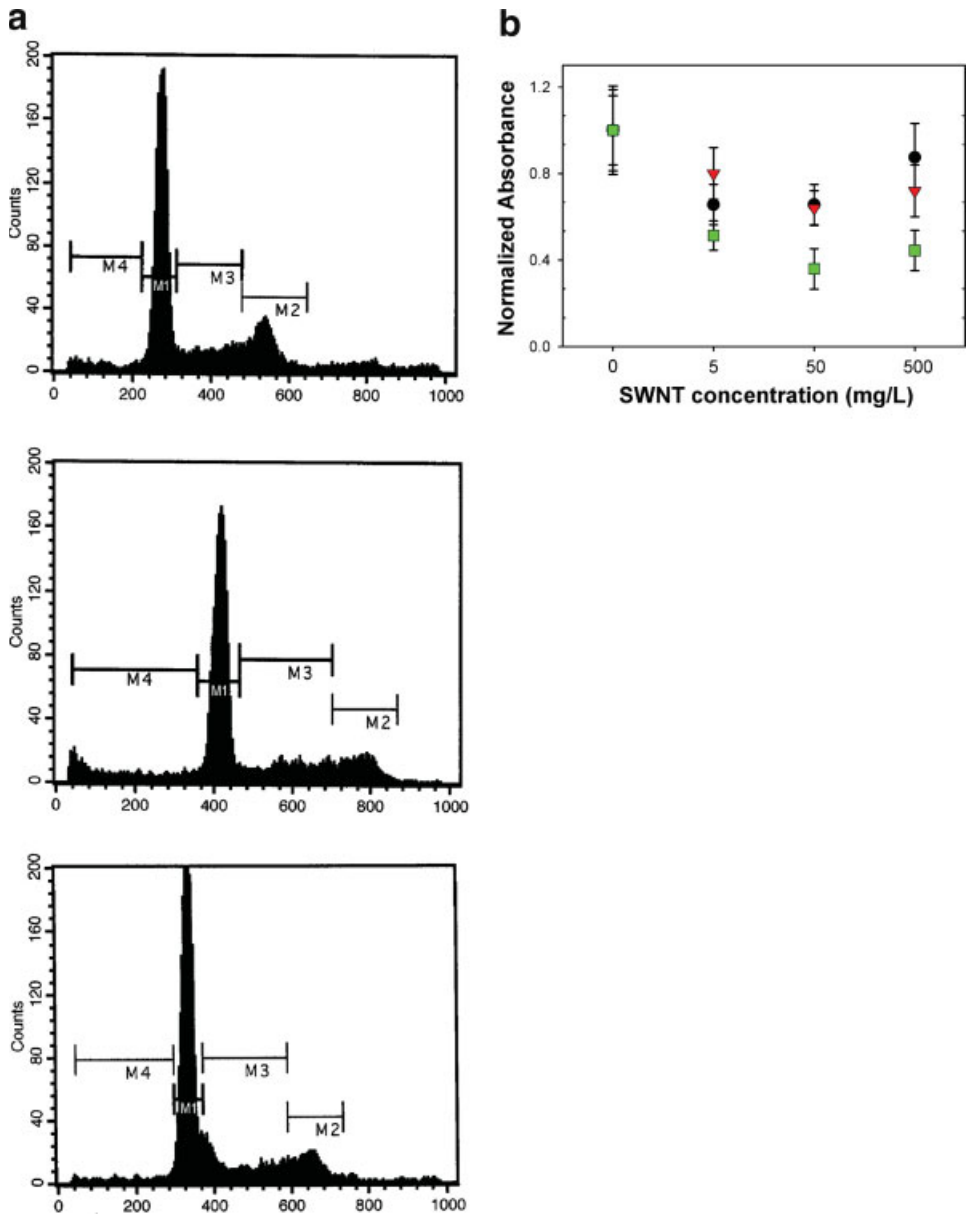

FIGURE 2. (a) Representative propidium iodide/fluorescence-activated cell sorter (PI-FACS) analyses of Hep3B (top) and HepG2 human hepatocellular carcinoma cells (middle), and Panc-1 human pancreatic adenocarcinoma cells (bottom) that were grown for 24 hours with Kentera single-walled carbon nanotubes (SWNTs) at a dose of 500 mg/L. The cell cycle proportions (M1 indicates G_0/G_1-phase fraction of cells; M2, G_2M-phase fraction of cells; M3, S-phase fraction of cells; M4, nonviable cells) of each cell line were normal, and no cytotoxicity was observed with SWNT concentrations from 5 mg/L up to 500 mg/L compared with control cells (grown without SWNTs). (b) MTT (3-[4,5-dimethylthiazol-2-yl]-2, 5-diphenyltetrazolium bromide) assay of the same 3 human carcinoma cell lines cultured for 24 hours with SWNTs at the concentrations shown. When cells were cultured with SWNT solutions at concentrations up to 500 mg/L, there was no significant growth inhibition noted in the 2 human hepatocellular carcinoma cell lines (Hep3B, black dots; HepG2, red triangles). In contrast, Panc-1 pancreatic adenocarcinoma cells (green squares) cultured with SWNTs did have a significant reduction ($P < .01$; analysis of variance) in proliferation that was similar at all concentrations of SWNTs. However, this reduced proliferative capacity was reversible because once media containing SWNTs was removed from Panc-1 cells, these cells returned to baseline growth rates within 48 hours.

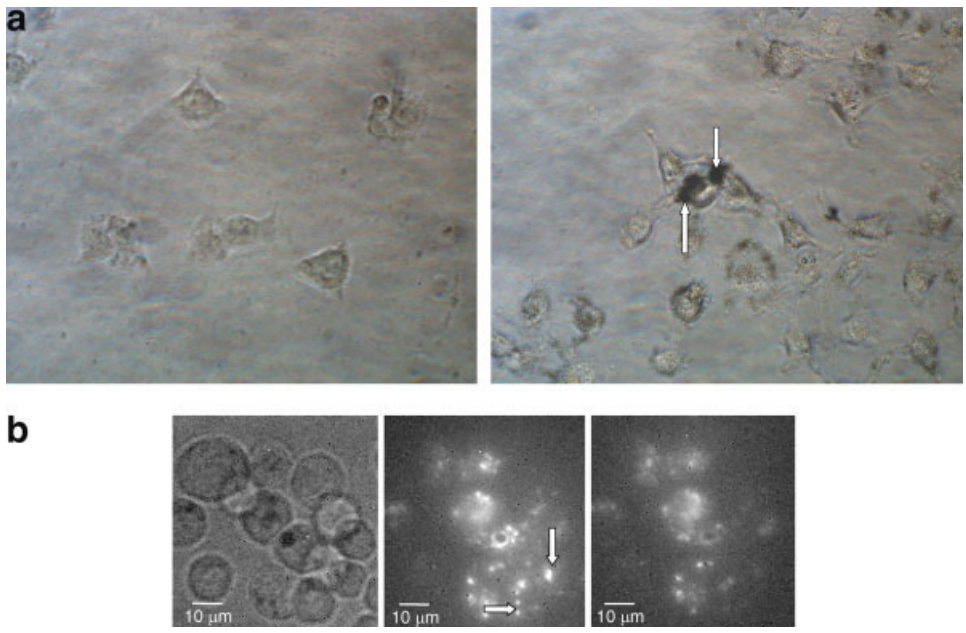

FIGURE 3. (a) Brightfield microscopic images demonstrate intracellular collections of single-walled carbon nanotubes (SWNTs) (arrows) (right) in Hep3B human hepatocellular carcinoma cells that were grown under standard culture conditions for 24 hours with Kentera SWNTs at a concentration of 500 mg/L. Similar intracellular collections of SWNTs were observed in HepG2 human hepatocellular carcinoma cells and in Panc-1 human pancreatic adenocarcinoma cells. Hep3B cells (left) were grown in media without SWNTs. (b) Near-infrared (IR), microscopic images of Kentera SWNTs in Panc-1 cells that were grown under standard culture conditions for 24 hours with SWNTs at a dose of 50 mg/L. A brightfield image is shown on the left, and the image in the center shows groups of fluorescent SWNTs in the cell cytoplasm and associated with the external cell membrane (arrows). An acid-washing procedure removed SWNTs adherent to the cell surface or present in the extracellular milieu, revealing numerous intracellular collections of near-IR SWNT fluorescence, as shown on the right (original magnification, ×60 in a and b).

5 mg/L. At any given concentration of SWNTs, the heating of the solutions was linear over time (Fig. 1a), and the heating rate increased linearly with RF generator output power (Fig. 1b). However, the heating rate of SWNT suspensions increased nonlinearly with increasing concentrations at any given RF power (Fig. 1c). Control experiments indicated that the heating rate of deionized water alone was 0.2 K per second, and the heating rate of Kentera polymer solutions alone was 0.7 K per second. Thus, the fractional heating provided by the SWNTs at the 50 mg/L concentration was 0.9 K per second, and the heating rate of Kentera SWNTs was 1.6 K per second. We observed that, at all concentrations of Kentera SWNT solutions, the Kentera polymer contributed ≈42% of the heating in the RF field. In all suspensions, the mass ratio of SWNTs to Kentera was 1:1.

Assessment of SWNT Toxicity In Vitro

Before determining the in vitro response of cells that had been incubated with SWNTs and treated with RF, we investigated potential cytotoxic effects of growing

FIGURE 4. (a) Graph demonstrating single-walled carbon nanotube (SWNT) concentration dependence in radiofrequency (RF) field-induced cytotoxicity in Hep3B (red bars), HepG2 (gold bars), and Panc-1 (blue bars) human cancer cells in vitro. All cell cultures received RF treatment at 800 watts (W) for 2 minutes. Cytotoxicity was determined by propidium iodide/fluorescence-activated cell sorter (PI-FACS) analysis. The values represent the mean ± standard error of the mean for experiments performed in triplicate. (b) Representative PI-FACS analysis of Hep3B hepatocellular carcinoma cells grown without SWNTs (control cells) (top) or grown with Kentera SWNTs (500 mg/L) (bottom). These cells were treated for 2 minutes in the RF field (800 W) and were processed for PI-FACS analysis 24 hours later. M1 indicates G_0/G_1-phase fraction of cells; M2, G_2M-phase fraction of cells; M3, S-phase fraction of cells; M4, nonviable cells. (c) Representative PI-FACS analysis of HepG2 hepatocellular carcinoma cells grown without SWNTs (control cells) (top) or grown with Kentera SWNTs (500 mg/L) (bottom). These cells were treated for 2 minutes in the RF field (800 W) and were processed for PI-FACS analysis 24 hours later. (d) Representative PI-FACS analysis of Panc-1 pancreatic carcinoma cells grown without SWNTs (control cells) (top) or grown with Kentera SWNTs (500 mg/L) (bottom panel). These cells were treated for 2 minutes in the RF field (800 W) and were processed for PI-FACS analysis 24 hours later.

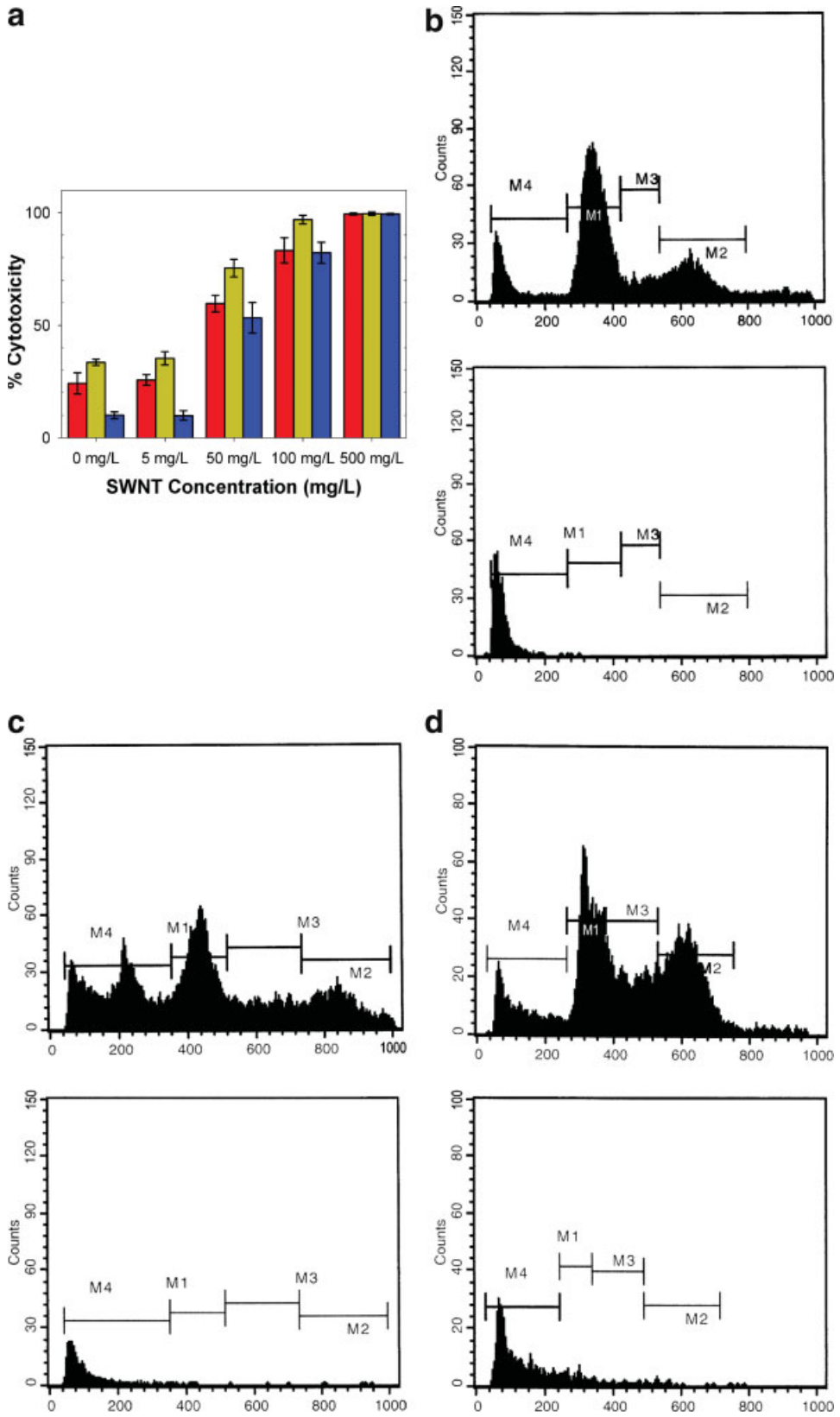
a
% Cytotoxicity
100
50
0
0 mg/L
5 mg/L
50 mg/L
100 mg/L
500 mg/L
SWNT Concentration (mg/L)
b
Counts
M4
M1
M3
M2
c
d

FIGURE 4

human cancer cells in the presence of various concentrations of SWNTs. There was no cytotoxicity in Hep3B, HepG2, or Panc-1 cells cultured for 6 to 48 hours with SWNTs in concentrations from 5 mg/L to 500 mg/L (Fig. 2a) compared with control cell cultures grown in the absence of SWNTs. MTT assays revealed no significant reduction in the proliferation of Hep3B or HepG2 cells grown with SWNTs in this same range of concentrations (Fig. 2b). However, there was a significant reduction ($P<.01$) in the proliferation of Panc-1 cells at all concentrations of SWNTs from 5 mg/L to 500 mg/L (Fig. 2b). This reduction in proliferation was reversible, because the Panc-1 cells that had been cultured in the presence of SWNTs demonstrated growth rates identical to control cells (no SWNT exposure) within 48 hours of removing SWNTs from the culture media. Brightfield microscopy revealed cytoplasmic collections of SWNTs in cells that had been incubated for 12 to 24 hours with SWNT concentrations of 50 mg/L, 100 mg/L, or 500 mg/L (Fig. 3a). Near-IR fluorescence microscopy confirmed the characteristic near-IR fluorescence of semiconducting SWNTs from the surface and the cytoplasm of the cells (Fig. 3b).

RF-induced Cytotoxicity of Cancer Cells In Vitro

Given these pronounced heating rates recorded in aqueous suspensions of SWNTs in an RF field, we tested the use of RF-induced SWNT heating to produce cancer cell cytotoxicity on 2 human hepatocellular cancer cell lines and 1 human pancreatic carcinoma cell line. In contrast to control conditions with no RF treatment, we observed SWNT concentration-dependent cellular cytotoxicity in vitro in all 3 cancer cell lines after 2 minutes of RF field exposure at 800 W of generator output power (Fig. 4a). At high concentrations of SWNTs (500 mg/L), cytotoxicity essentially was 100% in all 3 cell lines that had been exposed to the RF field for 2 minutes (Fig. 4b-d). It is worthy noting that control cell cultures containing only media or Kentera alone with no SWNTs had measurable rates of cell death (cytotoxicity rate, 11–35%) (Fig. 4a) that were significantly lower ($P < .01$) compared with the rates in cultures that containing SWNTs. No significant difference in cytotoxicity was observed when we compared the 2 groups of control cells (media alone or media with Kentera at concentrations up to 500 mg/L). However, SWNT-free cells that had been treated with RF at a generator output of 800 W for only 1 minute were completely viable. In contrast, 1 minute of RF exposure at 800 W in the 3 cancer cell lines containing SWNTs at 100 mg/L or 500 mg/L yielded cytotoxicity rates from 42% to 68% ($P < .01$ vs control cells). Thus, both SWNT concentration and duration of RF exposure are controlling factors for inducing cytotoxicity in vitro. The observed heating of the solute-rich cell culture media emphasizes the impact of nonspecific ionic stimulation with resultant heat production in a powerful RF field.

RF-induced Cytotoxicity of Malignant Liver Tumors In Vivo

Adult New Zealand white rabbits bearing VX2 tumors ranging in size from 1.0 cm to 1.3 cm in greatest dimension underwent a direct intratumoral injection of water-soluble SWNTs or control solutions. Immediately after injection of the SWNTs, the rabbits received 2 minutes of continuous RF treatment. After RF treatment, all animals were allowed to recover from anesthesia, and they were killed 48 hours later. The animals demonstrated no toxic effects from the injection of SWNTs or the RF treatment. Histopathology sections from tumors injected with SWNTs revealed complete thermal necrosis of the tumor tissue with a surrounding 2 mm to 5 mm zone of thermal injury to the liver (Fig. 5a). The remaining liver and all other organs that were assayed had no evidence of thermal injury or other abnormalities. In contrast, tumors that received injection of control solutions (Kentera alone, no SWNTs) followed by RF treatment had no evidence of tumor cell death in the histologic specimens (Fig. 5b). Tumors that had been injected with SWNTs but not treated with RF also were completely viable, as were tumors that had not been injected with SWNTs or control solutions and had been treated with RF alone (data not shown).

DISCUSSION

The substantial RF-induced heating rates of aqueous SWNT suspensions raises a critical question: How does a relatively small concentration of nanotubes (5–500 mg/L) significantly enhance RF-induced heating of the sample or the cancer cells? Because the RF wavelength (approximately 22 m for the frequency 13.56 MHz) greatly exceeds the nanotube length by approximately 300 nm to 1 μm, RF fields appear far off from any conceivable resonance,[14] and RF energy is much too small to excite electronic transitions in the semiconducting SWNTs. A possible simple explanation may be based on the resistive conductivity of the SWNTs and their high aspect ratios (length of individual SWNT/greatest dimension of individual SWNT).[15] Individual SWNTs, which typically measure 1 nm in greatest dimension, have an aspect ratio of approximately 300 to 1000. Thus, for example, for SWNTs that measure 1 μm in length at a concentration of 50 mg/L with a peak RF field strength of

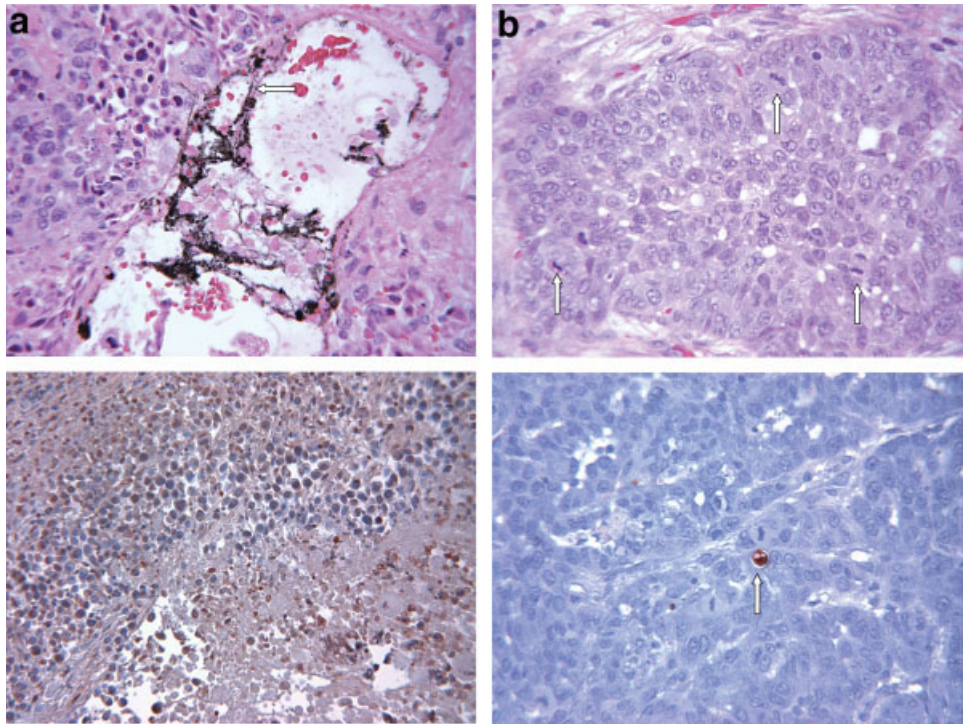

FIGURE 5. (a) Photomicrographs of hepatic VX2 tumors from rabbits that received intratumoral injection of Kentera single-walled carbon nanotubes (SWNTs) followed immediately by 2 minutes of radiofrequency (RF) field treatment. The top left photomicrograph demonstrates necrotic tumor cells, inflammatory cells, and long collections of coalesced SWNTs (black strands, arrow; standard H & E stain; original magnification, ×400); and the bottom left photomicrograph demonstrates the characteristic brown staining observed with apoptotic and necrotic cells (stained with terminal deoxynucleotidyl transferase biotin-deoxyuridine triphosphate nick-end labeling [TUNEL]; original magnification, ×250). (b) Photomicrographs of hepatic VX2 tumors from rabbits that received intratumoral injection of Kentera alone (no SWNTs) followed immediately by 2 minutes of RF field treatment. The top right photomicrograph demonstrates completely viable-appearing tumor cells with numerous mitotic bodies (arrows; standard H&E stain; original magnification, ×400), and the bottom right photomicrograph demonstrates the viable cells with only a rare brown apoptotic cell (arrow; stained with TUNEL; original magnification, ×400). The rate of apoptosis in untreated VX2 tumors was from 2% to 3%, and the control tumors treated with RF but no SWNTs had a similar 2% to 3% incidence of apoptotic cells.

approximately 15 kV/m, the predicted heating rate is 0.4 K per second, which is of the same order as the observed thermal contribution from SWNTs at this concentration and field strength in our system of approximately 0.9 K per second. One explanation for the larger observed (compared with the predicted) heating rate may be attributed to the dynamic self-assembly of the SWNTs into longer nanoantennae microns in length (effectively, greater length) under the influence of the RF field. The formation of self-assembled antennae of suspended SWNTs in an RF field is not the only potential explanation for higher than predicted heating rates in solutions, but at least a partial role for such a mechanism is supported by our observation of linear assembly of nonfunctionalized SWNT dispersions along the axis of the RF field (data not shown). The unique combination of high-field RF and aqueous SWNT suspensions used in the current study produced thermal effects that, to our knowledge, have not been reported previously.

Our results demonstrate that SWNTs can be used as a therapeutic agent to treat malignant tumors through RF-induced thermoablation, not just as a vector for the delivery of anticancer agents. From a clinical perspective, it is important that mammalian cancer cells generally are more sensitive to heat-induced damage and apoptosis than normal cells.[16] This advantage must be exploited when using this high-field external RF system to assure lethal thermal injury in malignant cells while sparing normal cells. We studied RF-induced heating of SWNTs in 2 human hepatocellular cell lines (Hep3B and HepG2) and in 1 pancreatic cancer cell line (Panc-1) in vitro. These cell lines were chosen in this initial study for 2 reasons: First, the liver is a common site for treatment with invasive RFA approaches; and, second, these types of cancer are particularly aggressive and resistant to standard cancer therapies, with locally advanced disease precluding potentially curative treatment in most patients.[17,18] Thus, these types of

cancer may be ideal for external RF therapy combined with the targeted delivery of SWNTs.

Studies that measure the concentrations of intracellular SWNTs needed for selective RF destruction of cancer cells will be critical in determining SWNT dosing schemes for targeted therapies. Because our data indicate that RF-induced heating of intracellular SWNTs is dose-dependent, methods to enhance cell-specific delivery and uptake of SWNTs will be crucial. SWNTs most likely enter normal and malignant cells through endocytosis.[8] SWNTs can be functionalized with several types of molecules to maintain stable hydrophilicity, but pegylation or use of noncovalent linkers such as Kentera offer the advantage of providing multiple binding sites for potential tumor targeting molecules.[19] Ideally, functionalized SWNTs can be targeted to cancer cells by covalently or noncovalently linking antibodies, peptides, carbohydrates, or pharmacologic agents directed at target molecules that are expressed or over expressed on cancer cells, as reported recently.[19]

Direct intratumoral injection of SWNTs or other agents in vivo is a minimally invasive but nonspecific approach, with RF-induced thermal injury to the tumor and adjacent normal tissue a predictable outcome. We observed thermal damage to normal liver parenchyma cells in a 3- to 5-mm zone around the VX2 tumors that were injected with SWNTs and then treated in the RF field. Nonspecific thermal injury to normal (nonmalignant) tissues and structures is associated with complications that arise in approximately 10% of patients who undergo invasive RFA treatment for malignant liver tumors.[20] Incomplete thermal destruction of the malignant cells also is possible with intratumoral injection because of uncontrollable heterogeneous SWNT concentrations throughout the tumor microenvironment. This again underscores the importance of developing cancer cell-specific targeting methods to minimize damage to normal cells while maximizing thermal-induced cancer cell cytotoxicity.

The absence of SWNT-related toxicity and no or minimal growth inhibition in the 3 human cancer cell lines we studied is consistent with other reports, in which no toxic irreversible effects were observed, even at high concentrations, from aqueous SWNT formulations in a variety of normal and malignant cell types.[8,10,21] Although an absence of acute toxicity after intravenous dosing of SWNTs has been documented in preclinical studies,[22,23] the complete safety of SWNTs in animals or humans cannot be assumed. Long-term studies to evaluate possible chronic toxicities associated with intravenous dosing of SWNTs must be performed in preclinical models.

Other investigators are evaluating the use of SWNTs and other nanoparticles as therapeutic targets to produce thermal injury to cancer cells. It is known that SWNTs absorb NIR light (range, 700–1600 nm), and continuous exposure to NIR light causes heat release by the SWNTs.[10] It has been demonstrated that this thermal property produced death in vitro in cancer cells with internalized SWNTs that were exposed to 2 minutes of continuous 808-nm NIR light at approximately 3.5 W/cm.[2,10] Unfortunately, this treatment approach is limited for use primarily in superficial malignant tumors because of the minimal tissue penetration (depth, <2–3 cm) by NIR-wavelength light.[24] This limitation is shared with treatments that are based on NIR heating of gold-silica nanoshell particles.[25] Electromagnetic heating of targeted nanoparticles avoids this issue; indeed, deep tissue tumor thermoablation injecting from 10 to 20 nm iron oxide particles (magnetite) has been reported.[26] It may be possible to achieve nonspecific targeting of malignant tumors by using magnetic focusing of these particles; however, some magnetite particles also may deposit in normal peritumoral tissue, leading to thermal destruction of both malignant and normal cells. A key metric for particle-based thermoablation treatments is the thermal power deposited per gram of receptor material. The highest value previously reported was 500 W/g for 15 nm maghemite (γ-Fe_20_3) colloids stimulated with 410 kilohertz AC magnetic fields at 11 kA/m.[27] We observed that 50 mg/L Kentera SWNT suspensions heated at a rate of 1.6 K per second when they were excited with 600 W of RF generator output power at 13.56 MHz in our system, yielding a rather remarkable total thermal power deposition of approximately 130,000 W/g. The heating rate attributable to the SWNTs in our experimental conditions was approximately 0.9 K per second, as noted above; this represents a thermal power deposition of approximately 75,000 W/g.

The results of the current study strongly suggest that the development of targeted delivery of SWNTs to malignant cells in vitro and in preclinical models should be investigated rigorously to determine whether there is a role for noninvasive RF treatment to effect the thermal destruction of malignant cells. Ultimately, we hope that such research will lead to our objective of initiating clinical trials using this approach in cancer patients.

REFERENCES

1. Haemmerich D, Laeseke PF. Thermal tumour ablation: devices, clinical applications and future directions. *Int J Hyperthermia*. 2005;21:755–760.

2. Bernardi P, Cavagnaro M, Pisa S, Piuzzi E. Specific absorption rate and temperature elevation in a subject exposed in the far-field of radio-frequency sources operating in the 10–900-MHz range. *IEEE Trans Biomed Eng*. 2003;50:295–304.
3. Iijima S. Helical microtubules of graphitic carbon. *Nature*. 1991;354:56–58.
4. Baughman RH, Zakhidov AA, de Heer WA. Carbon nanotubes—the route toward applications. *Science*. 2002;297: 787–792.
5. Bachtold A, Fuhrer MS, Plyasunov S, et al. Scanned probe microscopy of electronic transport in carbon nanotubes. *Phys Rev Lett*. 2000;84(26 pt 1):6082–6085.
6. McEuen PL, Fuhrer MS, Park H. Single-walled carbon nanotube electronics. *IEEE Trans Nanotech*. 2002;1:78–85.
7. Durkop T, Getty SA, Cobas E, Fuhrer MS. Extraordinary mobility in semiconducting carbon nanotubes. *Nano Lett*. 2004;4:35–39.
8. Bachilo SM, Strano MS, Kittrell C, et al. Structure-assigned optical spectra of single-walled carbon nanotubes. *Science*. 2002;298:2361–2366.
9. Zhang Z, Yang X, Zhang Y, et al. Delivery of telomerase reverse transcriptase small interfering RNA in complex with positively charged single-walled nanotubes suppresses tumor growth. *Clin Cancer Res*. 2006;12:4933–4939.
10. Kam NW, O'Connell M, Wisdom JA, Dai H. Carbon nanotubes as multifunctional biological transporters and near-infrared agents for selective cancer cell destruction. *Proc Natl Acad Sci USA*. 2005;102:11600–11605.
11. Kam NW, Liu Z, Dai H. Functionalization of carbon nanotubes via cleavable disulfide bonds for efficient intracellular delivery of siRNA and potent gene silencing. *J Am Chem Soc*. 2005;127:12492–12493.
12. Chen J, Liu H, Weimer WA, Halls MD, Waldeck DH, Walker GC. Noncovalent engineering of carbon nanotube surfaces by rigid, functional conjugated polymers. *J Am Chem Soc*. 2002;124:9034–9035.
13. Durney CH, Massoudi H, Iskander MF. Radiofrequency Radiation Dosimetry Handbook. 4th ed. Brooks AFB, Tex: U.S. Air Force School of Aerospace Medicine Press; 1986.
14. Sandler JKW, Kirk JE, Kinloch IA, Shaffer MSP, Windle AH. Ultra-low electrical percolation threshold in carbon-nanotube-epoxy composites. *Polymer*. 2003;44:5893–5899.
15. Landau LD, Lifshitz EM. Electrodynamics of Continuous Media. Oxford, United Kingdom: Elsevier; 2004.
16. Kampinga HH. Cell biological effects of hyperthermia alone or combined with radiation or drugs: a short introduction to newcomers in the field. *Int J Hyperthermia*. 2006;22:191–196.
17. Engstrom PF, Sigurdson ER, Evans A, Lewis N. Primary neoplasms of the liver. In: Kufe DW, Bast RC, Hait WN, et al., editors. Cancer Medicine. Volume 7. Hamilton, Ontario: B.C. Decker; 2006:1292–1301.
18. Wolff RA, Crane CH, Li D, Abruzzese JL, Evans DB. Neoplasms of the exocrine pancreas. In: Kufe DW, Bast RC, Hait WN, et al., editors. Cancer Medicine. Volume 7. Hamilton, Ontario: B.C. Decker; 2006:1331–1358.
19. Liu Z, Cai W, He L, et al. In vivo biodistribution and highly efficient tumor targeting of carbon nanotubes in mice. *Nat Nanotech*. 2007;2:47–52.
20. Curley SA, Marra P, Beaty K, et al. Early and late complications after radiofrequency ablation of malignant liver tumors in 608 patients. *Ann Surg*. 2004;239:450–458.
21. Dumortier H, Lacotte S, Pastorin G, et al. Functionalized carbon nanotubes are non-cytotoxic and preserve the functionality of primary immune cells. *Nano Lett*. 2006;6:1522–1528.
22. Cherukuri P, Gannon CJ, Leeuw TK, et al. Mammalian pharmacokinetics of carbon nanotubes using intrinsic near-infrared fluorescence. *Proc Natl Acad Sci USA*. 2006; 103:18882–18886.
23. Singh R, Pantarotto D, Lacerda L, et al. Tissue biodistribution and blood clearance rates of intravenously administered carbon nanotube radiotracers. *Proc Natl Acad Sci USA*. 2006;103:3357–3362.
24. Huang X, El-Sayed IH, Qian W, El-Sayed MA. Cancer cell imaging and photothermal therapy in the near-infrared region by using gold nanorods. *J Am Chem Soc*. 2006;128: 2115–2120.
25. Zhu TC, Finlay JC, Hahn SM. Determination of the distribution of light, optical properties, drug concentration, and tissue oxygenation in-vivo in human prostate during motexafin lutetium-mediated photodynamic therapy. *J Photochem Photobiol B*. 2005;79:231–241.
26. Hilger I, Hergt R, Kaiser WA. Towards breast cancer treatment by magnetic heating. *J Magnetism Magnetic Materials*. 2005;293:314–319.
27. Hergt R, Hiergeist R, Hilger I, et al. Maghemite nanoparticles with very high AC-losses for application in RF-magnetic hyperthermia. *J Magnetism Magnetic Materials*. 2004; 270:345–357.